Structure, Physical and Photophysical Properties, and Charge Separation Studies of $Re(bpm)(CO)_3L^{n+}$ Complexes (L = CH_3CN, py, MeQ^+, py-PTZ)

Randy J. Shaver,[†] Marc W. Perkovic,[†,‡] D. Paul Rillema,*[,†,‡] and Clifton Woods[§]

Departments of Chemistry, The University of North Carolina at Charlotte, Charlotte, North Carolina 28223, and The University of Tennessee, Knoxville, Tennessee 37996

Received March 22, 1995[⊗]

The synthesis, structure, and physical and/or photophysical properties of $Re(bpm)(CO)_3L^{n+}$, where bpm is 2,2′-bipyrimidine and L = CH_3CN, py (pyridine), MeQ^+ (*N*-methyl-4,4′-bipyridinium ion), and py-PTZ (10-(4-picolyl)-phenothiazine), are described. The structure of $[Re(bpm)(CO)_3(CH_3CN)]PF_6 \cdot {}^1/_2CH_3CN$ was determined by single-crystal X-ray diffraction. It crystallized in the space group $P\bar{1}$ with cell dimensions a = 10.089(11) Å, b = 11.855(6) Å, c = 18.990(6) Å, α = 89.71(3)°, β = 77.66(6)°, γ = 65.83(6)°, Z = 4, and D_{calcd} = 2.082 g/cm^3. Of the 5565 reflections (Mo Kα, 3.5° ≤ 2θ ≤ 45°), 4721 reflections with $F_o > 3.0\sigma(F_o)$ were used in full-matrix least-squares refinement. Final residuals were $R(F)$ = 0.0692 and $R_w(F)$ = 0.1026. The asymmetric unit contained two independent cations. The Re−N(bpm) bond distances were 2.171(9) and 2.198(10) Å for one cation and 2.161(12) and 2.187(12) Å for the other; the two Re−N(CH_3CN) bond distances were 2.094(14) and 2.177(13) Å, and the Re−C(CO) bond distances were 1.908(15), 1.938(17), and 1.912(12) Å for the first cation and 1.897(15), 1.896(19), and 1.919(15) Å for the second. The complexes exhibited three CO infrared-active bands in the 1900−2100 cm^{-1} region and underwent optical transitions in the 300−350 nm region assigned to dπ(Re) → π^*(bpm) transitions and in the 200−300 nm region assigned to intraligand $\pi \rightarrow \pi^*$ transitions. The complexes underwent multiple reductions attributed to reduction of coordinated bpm and MeQ^+. The first reduction of $Re(bpm)(CO)_3py^+$ was located at $E_{1/2}$ = −0.84 V vs SSCE, whereas the first reduction of $Re(bpm)(CO)_3MeQ^{2+}$ was observed at $E_{1/2}$ = −0.70 V vs SSCE and was attributed to reduction of the MeQ^+ ligand. The only oxidations observed were for $Re(bpm)(CO)_3py\text{-}PTZ^+$. These were located at $E_{1/2}$ values of 0.82 and 1.53 V vs SSCE and were attributed to oxidation of the py-PTZ ligand. Emission was observed from all the complexes in acetonitrile at room temperature except from $Re(bpm)(CO)_3py\text{-}PTZ^+$. The emission quantum yields were low (Φ_{em} = (0.5−2) × 10^{-3}) and the emission lifetimes were short ($\tau \sim 2$ ns). Transient absorption spectra revealed that charge separation occurred for both $Re(bpm)(CO)_3MeQ^{2+}$ and $Re(bpm)(CO)_3py\text{-}PTZ^+$ and involved transfer of an electron from Re(I) to MeQ^+ generating Re(II) and the $MeQ^\bullet$ radical in the former and from py-PTZ to Re(II) forming the py-PTZ^+ radical cation and Re(I) in the latter. Intramolecular back electron transfer in $[(bpm^-)Re^{I}(CO)_3(py\text{-}PTZ^+)]^+$ occurred at a rate of 1.6 × 10^8 s^{-1} and in $[(bpm)Re^{II}(CO)_3(MeQ^\bullet)]^{2+}$ at a rate of 5.5 × 10^7 s^{-1}.

Introduction

The role of charge separation is fundamental in photosynthesis, and various models based on transition metal complexes have been designed in attempts to emulate the process. One reported model system is based on quinone electron acceptor units attached via covalent linkages to porphyrin ligands.[1] Another approach has taken advantage of ligands that, when attached to a transition metal, can either donate an electron to or accept an electron from a luminophore upon photoexcitation.[2−4]

The latter approach is the one taken in this report. The photophysical properties of $Re(bpm)(CO)_3L^{n+}$, where bpm is 2,2′-bipyrimidine and L is either the electron-accepting ligand *N*-methyl-4,4′-bipyridinium (MeQ^+) or the electron-donating ligand 10-(4-picolyl)phenothiazine (py-PTZ), are compared to those of the models $Re(bpm)(CO)_3py^+$ and $Re(bpm)(CO)_3(CH_3CN)^+$. The structures of the various ligands are shown in Figure 1. Equation 1 illustrates the charge transfer step normally

$$(bpm)Re^{I}(CO)_3L^+ \xrightarrow{h\nu} (bpm^-)Re^{II}(CO)_3L^{+*} \qquad (1)$$

associated with initial photoexcitation for Re(I) polypyridyl complexes.[5−13] However, for L = MeQ^+, the π^* energy level on MeQ^+ may be lower in energy than that for L = py, such that its population (eq 2) may compete with the process in eq

[†] The University of North Carolina at Charlotte.
[‡] Current address: Department of Chemistry, Wichita State University, Wichita, KS 67260−0051.
[§] The University of Tennessee.
[⊗] Abstract published in *Advance ACS Abstracts,* October 1, 1995.

(1) For a review see: Connolly, J. S.; Bolton, J. R. In *Photoinduced Electron Transfer*; Fox, M. A., Chanon, M., Eds.; Elsevier: Amsterdam, 1988; Part D, pp 303−393 and references therein.
(2) Chen, P.; Curry, M.; Meyer, T. J. *Inorg. Chem.* **1989**, *28*, 2271.
(3) Chen, P.; Westmoreland, T. D.; Danielson, E.; Schanze, K. S.; Anthon, D.; Neveux, P. E., Jr.; Meyer, T. J. *Inorg. Chem.* **1987**, *26*, 1116.
(4) Ryu, C. K.; Wang, R.; Schmehl, R. H.; Ferrane, S.; Ludwikow, M.; Merkert, J. W.; Headford, C. E. L.; Elliott, C. M. *J. Am. Chem. Soc.* **1992**, *114*, 430.
(5) Geoffroy, G. L.; Wrighton, M. S. *Organometallic Photochemistry*; Academic Press: New York, 1979.
(6) Lees, A. J. *Chem. Rev.* **1987**, *87*, 711.
(7) Kalyanasundaram, K. *Photochemistry of Polypyridine and Porphyrin Complexes*; Academic Press: New York, 1992.
(8) Meyer, T. J. *Pure Appl. Chem.* **1986**, *58*, 1193.
(9) (a) Van Wallendael, S.; Shaver, R. J.; Rillema, D. P.; Yoblinski, B. J.; Stathis, M.; Guarr, T. F. *Inorg. Chem.* **1990**, *29*, 1761. (b) Sahai, R.; Rillema, D. P.; Shaver, R. J.; Van Wallendael, S.; Jackman, D. C.; Boldaji, M. *Inorg. Chem.* **1989**, *28*, 1022.
(10) Ruminski, R.; Cambron, R. T. *Inorg. Chem.* **1990**, *29*, 1574.
(11) Baiano, J. A.; Carlson, D. L.; Wolosh, G. M.; DeJesus, D. E.; Knowles, C. F.; Szabo, E. G.; Murphy, W. R., Jr. *Inorg. Chem.* **1990**, *29*, 2327.
(12) Wallace, L.; Rillema, D. P. *Inorg. Chem.* **1993**, *32*, 3836.
(13) (a) Sacksteder, L.; Zipp, A. P.; Brown, E. A.; Streich, J.; Demas, J. N.; DeGraff, B. A. *Inorg. Chem.* **1990**, *29*, 4335. (b) Leasure, R. M.; Sacksteder, L.; Nesselrodt, D.; Reitz, G. A.; Demas, J. N.; DeGraff, B. A. *Inorg. Chem.* **1991**, *30*, 3722.

0020-1669/95/1334-5446$09.00/0

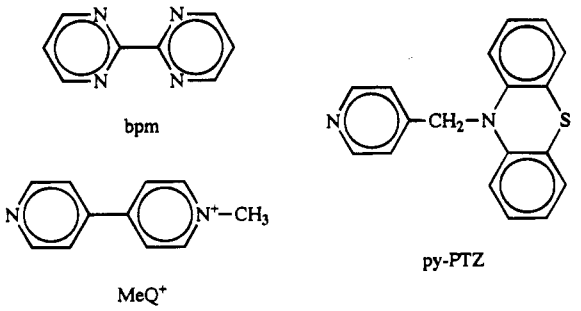

Figure 1. Ligands 2,2′-bipyrimidine (bpm), *N*-methyl-4,4′-bipyridinium (MeQ^+), and 10-(4-picolyl)phenothiazine (py-PTZ).

$$(bpm)Re^{I}(CO)_3(MeQ^+)^{2+} \xrightarrow{h\nu} (bpm)Re^{II}(CO)_3(MeQ^{\bullet})^{+\bullet} \quad (2)$$

1. In this report, we examine this issue and compare it to the case where the electron-donor ligand py-PTZ is attached to the $(bpm)Re(CO)_3^+$ framework.

Experimental Section

Materials. $Re(CO)_5Cl$ was purchased from Pressure Chemical Co. and was used without further purification. The ligand 2,2′-bipyrimidine (bpm) was purchased from Aldrich and was used without further purification. Tetrabutylammonium hexafluorophosphate (TBAH) was purchased as Electrometric Grade from Southwestern Analytical Chemicals, Inc., and was stored under vacuum. Silver trifluoromethanesulfonate (silver triflate) and silver hexafluorophosphate were purchased commercially, stored in the absence of light in a vacuum desiccator, and used without any further purification. Methanol, acetonitrile, methylene chloride, and acetone were HPLC grade. Acetonitrile used in the electrochemistry experiments was dried over 4 Å molecular sieves.

Preparation of Compounds. The compounds $[Re(bpm)(CO)_4](CF_3SO_3)$ and $Re(bpm)(CO)_3Cl$ were available from previous studies.[9,14] The compound 10-(4-picolyl)phenothiazine (py-PTZ) was provided by Professor T. J. Meyer's group at The University of North Carolina at Chapel Hill.

***N*-Methyl-4,4′-bipyridinium Hexafluorophosphate, $(MeQ)PF_6$.** The preparative method used was one reported by Tabushi and Yazaki.[15] 4,4′-Bipyridine dihydrate (3.02 g; 15.7 mmol) was placed in 200 mL of acetonitrile, and the mixture was heated until the solid dissolved (approximately 60 °C). Methyl iodide (2.23 g; 15.7 mmol) was dissolved in 30 mL of acetonitrile. This solution was then added dropwise over a 4 h time period from an addition funnel to the bipyridine solution which was maintained at 60 °C. After an additional 5 h, an orange precipitate was collected by suction filtration (paraquat). The yellow filtrate was reduced to dryness using a rotary evaporator and redissolved in water; a saturated solution of ammonium hexafluorophosphate was added to the solution to yield a white precipitate. The white precipitate was collected by suction filtration. Yield = 3.04 g (9.62 mmol; 61.2%). CV (volts vs SSCE): −0.98 V (80 mV) and −1.66 V (85 mV). ^{1}H NMR (acetone-d_6): δ 4.65 (s), 7.96 (dd; J = 4.5, 1.8 Hz), 8.63 (d; J = 6.6 Hz), 8.86 (dd; J = 4.5, 1.8 Hz), 9.20 (d; J = 6.9 Hz).

$Re(CO)_5(CF_3SO_3)$. $Re(CO)_5Cl$ (1.00 g; 2.77 mmol) was dissolved in 50 mL of methylene chloride, and silver triflate (0.780 g; 3.04 mmol) was added to the solution. The resultant solution was stirred overnight under argon in the dark. A white precipitate (AgCl) formed and was removed by suction filtration. The filtrate was evaporated to dryness, leaving the desired white solid. Yield = 1.12 g (2.36 mmol; 85.4%). Anal. Calcd: C, 15.16; H, 0.0; N, 0.0. Found: C, 14.99; H, 0.0; N, 0.0.

$Re(bpm)(CO)_3py(CF_3SO_3)\cdot H_2O$. A 25 mL round-bottom flask was charged with a solution of $Re(bpm)(CO)_4(CF_3SO_3)$ (80 mg; 0.0132 mmol) in pyridine (~4 mL). The mixture was heated at reflux under argon and stirred in the dark for 18 h. The crude product was precipitated by the addition of ~15 mL of ethyl ether. This product was then dissolved in methylene chloride (~15 mL), sorbed onto a neutral alumina column (1 × 10 cm), washed with methylene chloride, and eluted with acetonitrile. One yellow fraction was collected, and one yellow, luminescent band remained at the top of the column. The yellow fraction was evaporated to dryness. This solid was dissolved in methylene chloride and reprecipitated by adding hexane. The yellow product was collected by suction filtration. Yield = 52 mg (0.00771 mmol; 58.4%). Anal. Calcd: C, 30.27; H, 1.94; N, 10.38. Found: C, 30.42; H, 1.88; N, 10.46.

$Re(bpm)(CO)_3(CH_3CN)(CF_3SO_3)$. A 100 mL round-bottom flask was charged with $Re(bpm)(CO)_4(CF_3SO_3)$ (102 mg; 0.00169 mmol) and ~60 mL of acetonitrile. The mixture was refluxed under argon in the dark for 3 days. The resultant solution was reduced in volume to approximately 3 mL, and the desired complex precipitated upon addition of ethyl ether. The crude product was dissolved in 5 mL of methylene chloride, sorbed onto a neutral alumina column (1 × 10 cm), washed with methylene chloride, and then eluted with acetonitrile. A yellow fraction was collected and evaporated to dryness. The solid remaining in the flask was dissolved in methylene chloride, yielding a yellow precipitate upon the addition of hexane. Yield = 74 mg (0.0120 mmol; 70.9%). Anal. Calcd: C, 27.19; H, 1.47; N, 11.32. Found: C, 27.09; H, 1.50; N, 11.27.

$Re(bpm)(CO)_3(MeQ)(PF_6)_2$. A 100 mL round-bottom flask was charged with 200 mg (0.0553 mmol) $Re(CO)_5Cl$ and ~40 mL of methylene chloride. $AgPF_6$ (152 mg; 0.0601 mmol) was dissolved in ~5 mL of methanol, and the solution was added to the flask. The mixture was stirred in the dark under argon for 18 h. The AgCl formed during this time was removed by suction filtration. The filtrate was placed in a 100 mL round-bottom flask, and bipyrimidine (140 mg; 0.0885 mmol) was added. The mixture was stirred in the dark under argon at room temperature for 10 h. The resulting solution was evaporated to dryness, and ~25 mL of methanol was added to dissolve the remaining solids. The solution was then filtered and again evaporated to dryness. The solid material remaining in the flask was dissolved in ~50 mL of methylene chloride, the solution was placed in a 100 mL round-bottom flask containing 92.5 mg of $MeQ(PF_6)$ (0.0292 mmol) dissolved in ~5 mL of methanol, and the mixture was stirred in the dark for 18 h at room temperature under argon. The solution was then evaporated to dryness. The solid material remaining in the flask was dissolved in a minimal amount of acetone and precipitated by addition of ethyl ether. The product was collected by suction filtration and dried under vacuum. Yield = 96 mg (0.0108 mmol; 37%). Anal. Calcd C, 29.77; H, 1.93; N, 9.45. Found: C, 29.52; H, 2.00; N, 9.40.

$Re(bpm)(CO)_3(py\text{-}PTZ)(PF_6)$. A 100 mL round-bottom flask was charged with 250 mg of $Re(CO)_5Cl$ (0.0691 mmol) and ~40 mL of methylene chloride. $AgPF_6$ (178 mg; 0.0704 mmol) dissolved in 5 mL of methanol was added to the flask. The mixture was stirred in the dark under argon for 18 h. The AgCl that formed was then removed by suction filtration. The filtrate was placed in a 100 mL round-bottom flask, and 200 mg of bipyrimidine (0.126 mmol) was added. The mixture was stirred under argon in the dark at room temperature for 10 h. The resultant solution was evaporated to dryness by rotary evaporation, and about 25 mL of methanol was added to dissolve the product. The solution was filtered to remove insoluble materials, and the filtrate was again evaporated to dryness. The remaining product was dissolved in ~50 mL of methylene chloride, the solution was placed in a 100 mL round-bottom flask containing 150 mg of py-PTZ (0.0517 mmol) dissolved in 5 mL of methanol, and the mixture was stirred in the dark for 18 h at room temperature under argon. The solution was evaporated to dryness. The product was dissolved in a minimal amount of acetone, precipitated by dropwise addition of ethyl ether, collected by suction filtration, and dried in vacuo. Yield = 114 mg (0.0132 mmol; 25.5%). Anal. Calcd C, 40.33; H, 2.33; N, 9.73. Found: C, 40.19; H, 2.37; N, 9.66.

Physical Measurements. Ultraviolet−visible spectra were recorded with a Perkin-Elmer Model 3840 diode array spectrophotometer. Uncorrected emission spectra and luminescence intensity measurements were recorded using a Hitachi Perkin-Elmer Model 650-40 fluorescence spectrophotometer. Corrected emission spectra were obtained on a

(14) Shaver, R. J.; Rillema, D. P. *Inorg. Chem.* **1992**, *31*, 1401.
(15) Tabushi, I.; Yazaki, A. *Tetrahedron* **1981**, *37*, 4185.

SPEX Fluorolog 212 spectrofluorometer. The samples were equilibrated at 25 °C in a Haake Model FK2 constant-temperature bath before measurement.

Cyclic voltammograms were obtained under argon in a conventional H-cell containing acetonitrile, methylene chloride, or tetrahydrofuran with 0.1 M tetrabutylammonium hexafluorophosphate (TBAH) as the supporting electrolyte. A Pt disk served as the working electrode, and a Pt wire functioned as the counter electrode. Potentials were measured versus the saturated sodium chloride calomel electrode (SSCE). Electrochemistry was carried out with a PAR 174 polarographic analyzer or a PAR 173 potentiostat in conjunction with a PAR 175 programmer. The voltammograms were recorded with an IBM 7424 X-Y recorder.

Emission lifetimes were acquired using a previously described[16] single-photon-counting instrument located at the Notre Dame Radiation Laboratory and an in-house unit consisting of a Photochemical Research Associates Model LN1000 N_2 laser and a PAR LN102 dye laser as the excitation sources. The analog signal from the photomultiplier tube was digitized with a LeCroy 6010 transient digitizer system employing either a 6880A or a TR8828 transient recorder. The LeCroy 6010 was controlled by Catalyst software supplied by LeCroy. Emission lifetimes were calculated by the program LIFETIME described previously.[14]

Nanosecond and picosecond transient absorption measurements were performed on previously described instrumentation[17] located at the Notre Dame Radiation Laboratory. The nanosecond instrument used a frequency-tripled Nd:YAG as the pump (QuantaRay; 10 ns fwhm; ~3 mJ/pulse) and a pulsed Xe arc lamp as the probe. Spectra were measured in Ar-degassed CH_2Cl_2 in a 1 cm cuvette with 90° pump–probe beam geometry. All spectra were corrected for ground-state absorption. The picosecond instrument used a mode-locked Nd:YAG (Quantel) to generate both the pump (22 mJ/pulse at 355 nm) and the quasi-contiuum probe beams. Both beams shared a temporal resolution of 18 ps (fwhm), and the beams intersected a 1 cm curvette at an angle of 90°. Samples were prepared in Ar-degassed CH_2Cl_2. Measurements with both instruments were performed using flowing solutions. The independent variable for each instrument (wavelength for the nanosecond machine; time delay for the picosecond unit) was randomized for each experiment.

Emission quantum yields were calculated by a comparison to rhodamine B using eq 3,[18] where Φ_{em} is the experimental emission

$$\Phi_{em} = \frac{\eta_s^2 I_S A_0}{\eta_0^2 I_0 A_S}\Phi_0 \qquad (3)$$

quantum yield, I_0, A_0, and η_0 are respectively the emission intensity, absorbance of rhodamine B at the excitation wavelength, and the refractve index of the solvent; I_s, A_s, and η_s are respectively the emission intensity, absorbance, and index of refraction of the sample; Φ_0 is the emission quantum yield of rhodamine B (0.69 at λ_{ex} = 355 mm)[3] in ethanol at 25 °C.

Emission quantum yield and lifetime measurements were made on optically dilute samples having absorbances equal to or less than 0.1 at the excitation wavelength.

Collection and Reduction of X-ray Data. X-ray data were collected on a Nicolet R3m/V diffractometer using the $\theta-2\theta$ method. A total of 5565 reflections were recorded to a 2θ value of 45°. Of the 5565 reflections (Mo Kα, 3.5° ≤ 2θ ≤ 45°), 4721 reflections with $F_o > 3.0\sigma(F_o)$ were used in full-matrix least-squares refinement. Final residuals were $R(F) = 0.0692$ and $R_w(F) = 0.1026$. Data were corrected for Lorentz and polarization effects, and an empirical absorption correction based on the Φ dependence of five reflections with χ ca. 90° was applied (T_{max}:T_{min} = 0.854:0.378). The Re atoms were located by direct methods using Nicolet SHELXTL PLUS software,[19] and the remaining positions of non-hydrogen atoms were found by conventional difference Fourier techniques. Anomalous dispersion, correction, and scattering factors were obtained from ref 20. The structure was refined using a full-matrix least-squares adjustment of non-hydrogen positional and anisotropic thermal parameters. The hydrogen atoms were placed 0.96 Å away from attached carbon atoms and were not refined. The single-crystal X-ray crystallographic analysis data are given in Table 1.

Table 1. Crystallographic Data for $[Re(bpm)(CO)_3(CH_3CN)](PF_6)\cdot{}^1/_2CH_3CN$

$ReC_{14}H_{10.5}N_{5.5}F_6O_3P$	$\beta = 77.66(6)°$
space group = $P\bar{1}$	$\gamma = 65.83(6)°$
fw = 634.9	$Z = 4$
T = 295 K	d_{calc} = 2.082 g/cm^3
a = 10.089(11) Å	μ = 6.236 mm^{-1}
b = 11.855(6) Å	$R(F)^a$ = 0.0692
c = 18.990(6) Å	$R_w(F)^b$ = 0.1026
λ(Mo Kα) = 0.710 69 Å	V = 2015(2) Å^3
α = 89.71(3)°	

^{a} $R(F) = \sum||F_o| - |F_c||/\sum|F_o|$. ^{b} $R_w(F) = (\sum(||F_o| - |F_c||)^2/\sum|F_o|)^{1/2}$; $w^{-1} = \sigma^2(F_o) + 0.0048F_o^2$.

Scheme 1. Steps Used To Prepare MeQ^+ and py-PTZ Complexes

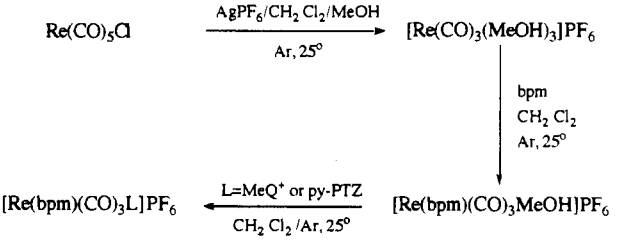

Results

Preparation of Compounds. Two methods were used to prepare the tricarbonyl complexes. The first involved thermal displacement of CO from $Re(bpm)(CO)_4^+$ as illustrated in eq 4. The mixture was refluxed until a change in color of the

$$Re(bpm)(CO)_4^+ \xrightarrow{S = CH_3CN \text{ or py}} Re(bpm)(CO)_3S^+ + CO \qquad (4)$$

luminescence (green to yellow) was observed by visual inspection under an ultraviolet lamp. The crude product was purified on a neutral alumina column, previously developed with methylene chloride, by eluting it with methanol.

The second procedure is illustrated in Scheme 1. Here, a series of steps were used to prepare the MeQ^+ and py-PTZ derivatives. These involved formation of a trimethanolate from $Re(CO)_5Cl$, conversion of the trimethanolate derivative to $Re(bpm)(CO)_3(CH_3OH)^+$, and then addition of the desired electron-donor or -acceptor ligand. The product was isolated as the PF_6^- salt and purified by recrystallization.

Structure of the Acetonitrile Adduct. The single-crystal (isolated from a 4:1 acetonitrile–toluene solution) X-ray crystallographic analysis positional parameters are given in Table 2. The asymmetric unit contains two Re cations, two PF_6^- anions, and an acetonitrile molecule. The geometry of one of the cations is illustrated in Figure 2, the coordination geometry of the second cation being nearly identical. Table 3 contains selected bond distances and angles for the two cations. The coordination geometry of the Re atoms is that of a slightly distorted octahedron. The distortion is caused by the small bite angle of the bpm ligands (average value of 74.9°). Each cation contains two types of CO ligands: one is *trans* to an acetonitrile molecule; the other is *trans* to a bpm ligating nitrogen atom.

(16) Federici, J.; Helman, W. P.; Hug, G. L.; Kane, C.; Patterson, L. K. *Comput. Chem.* **1985**, 9, 171.
(17) Ebbeson, T. W. *Rev. Sci. Instrum.* **1988**, *59*, 1307.
(18) Demas, J. N.; Crosby, G. A. *J. Phys. Chem.* **1971**, *75*, 991.
(19) Sheldrick, G. M. *SHELXTL PLUS*, version 4.1; Siemens Analytical X-Ray Instruments, Inc.: Madison, WI, 1990.
(20) *International Tables for X-Ray Crystallography*; Kynoch: Birmingham, England, 1974; Vol. IV.

Table 2. Atomic Coordinates ($\times 10^4$) and Equivalent Isotropic Displacement Coefficients (Å^2 $\times$ 10^3) for [Re(CO)$_3$(C$_8$H$_6$N$_4$)(CH$_3$CN)]PF$_6$·$^1/_2$CH$_3$CN

atom	x	y	z	U(eq)[a]
Re(1)	1799(1)	3420(1)	2764(1)	42(1)
Re(1A)	7821(1)	−6478(1)	984(1)	44(1)
C(1)	1280(15)	4440(13)	2000(8)	56(6)
O(1)	925(15)	4982(12)	1515(6)	84(7)
C(2)	3648(19)	2425(13)	2101(8)	57(7)
O(2)	4795(12)	1841(11)	1705(7)	80(5)
C(3)	1024(14)	2323(12)	2443(7)	48(6)
O(3)	631(12)	1639(10)	2254(6)	68(5)
C(1A)	7703(16)	−5834(13)	1916(8)	55(6)
O(1A)	7586(14)	−5471(11)	2516(7)	88(6)
C(2A)	7847(19)	−4990(15)	622(8)	68(8)
O(2A)	7874(21)	−4098(13)	389(8)	117(9)
C(3A)	5683(16)	−5710(13)	1221(9)	57(7)
O(3A)	4431(14)	−5293(11)	1352(8)	96(6)
N(1)	2085(12)	2460(9)	3749(5)	44(5)
C(6)	3260(19)	1380(14)	3774(9)	71(8)
C(7)	3246(20)	821(16)	4417(9)	76(8)
C(8)	2051(25)	1381(20)	4984(10)	87(11)
N(2)	905(17)	2448(13)	4955(6)	70(7)
C(9)	957(15)	2936(13)	4326(8)	55(7)
C(10)	−297(14)	4122(13)	4261(6)	45(6)
N(3)	−182(12)	4514(10)	3599(5)	49(5)
C(11)	−1312(14)	5580(12)	3501(8)	51(6)
C(12)	−2539(18)	6179(16)	4083(9)	76(8)
C(13)	−2537(20)	5705(17)	4734(9)	75(8)
N(4)	−1407(14)	4660(13)	4811(6)	63(6)
N(5)	2681(12)	4525(10)	3164(6)	49(5)
C(4)	3197(17)	5076(13)	3405(7)	58(6)
C(5)	3842(23)	5776(15)	3728(9)	80(9)
N(1A)	7939(12)	−7410(10)	−29(6)	50(5)
C(6A)	7901(16)	−6919(13)	−650(7)	54(6)
C(7A)	7922(19)	−7600(15)	−1264(8)	69(8)
C(8A)	8001(20)	−8781(15)	−1151(8)	71(8)
N(2A)	8077(15)	−9283(11)	−541(6)	61(6)
C(9A)	8084(14)	−8614(12)	−13(7)	47(6)
C(10A)	8137(12)	−9076(11)	718(7)	43(5)
N(3A)	7996(11)	−8299(10)	1256(6)	46(5)
C(11A)	7990(13)	−8757(13)	1905(6)	46(6)
C(12A)	8147(15)	−9959(14)	1992(7)	57(7)
C(13A)	8309(16)	−10661(13)	1432(7)	54(6)
N(4A)	8296(13)	−10262(10)	764(6)	59(5)
N(5A)	10244(15)	−7401(10)	671(6)	56(6)
C(4A)	11495(16)	−7907(14)	506(8)	59(7)
C(5A)	13109(16)	−8523(17)	302(9)	73(8)
P(1)	6881(5)	2137(4)	4177(2)	66(2)
F(1)	8064(19)	2394(19)	3601(8)	172(11)
F(2)	5711(20)	1824(15)	4707(9)	162(10)
F(3)	5738(15)	2623(12)	3685(8)	128(7)
F(4)	7987(19)	1599(16)	4674(8)	169(10)
F(5)	7525(15)	793(10)	3745(7)	130(7)
F(6)	6205(16)	3471(12)	4550(7)	118(7)
P(1A)	5207(5)	−1760(4)	2286(3)	78(2)
F(1A)	4702(18)	−2782(15)	2135(9)	145(10)
F(2A)	5648(16)	−702(12)	2516(10)	142(8)
F(3A)	3529(15)	−792(16)	2441(8)	146(8)
F(4A)	6932(15)	−2689(12)	2146(9)	145(8)
F(5A)	5430(23)	−1481(20)	1491(7)	174(13)
F(6A)	4981(18)	−2015(16)	3119(7)	138(10)
C(14)	9018(24)	936(24)	6194(12)	117(12)
C(15)	9309(23)	1644(24)	6652(13)	97(11)
N(6)	9607(26)	2222(24)	6976(11)	123(13)

[a] Equivalent isotropic U defined as one-third of the trace of the orthogonalized U_{ij} tensor.

The average length of the Re−C bond *trans* to the acetonitrile is 1.929 Å compared to the averages of 1.903 and 1.904 Å for the Re−C bond *trans* to the two bpm nitrogen atoms. The similar Re−CO bond distances reflect similar π-acceptor ability for the two types of CO ligands. There are also two types of nitrogen atoms: one from a coordinated acetonitrile; the other from the bpm ligand. The average Re−N bond distance to acetonitrile is 2.136 Å compared to average values of 2.166 and 2.193 Å to the bpm nitrogen atoms.

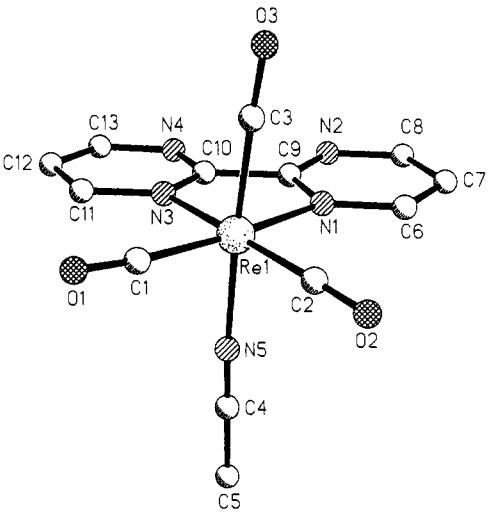

Figure 2. Structural drawing of one of the two independent Re(bpm)(CO)$_3$CH$_3$CN$^+$ cations in the asymmetric unit. The second cation shows a virtually identical coordination sphere.

Table 3. Selected Bond Distances and Angles for [Re(CO)$_3$(C$_8$H$_6$N$_4$)CH$_3$CN]PF$_6$·$^1/_2$CH$_3$CN

Bond Distances (Å)			
Cation 1			
Re(1)−C(1)	1.908(15)	Re(1)−C(2)	1.912(13)
Re(1)−C(3)	1.938(17)	Re(1)−N(1)	2.198(10)
Re(1)−N(3)	2.171(9)	Re(1)−N(5)	2.094(14)
C(1)−O(1)	1.157(19)	C(2)−O(2)	1.164(17)
C(3)−O(3)	1.132(22)	N(5)−C(4)	1.143(24)
C(4)−C(5)	1.459(31)		
Cation 2			
Re(1A)−C(1A)	1.897(15)	Re(1A)−C(2A)	1.896(19)
Re(1A)−C(3A)	1.919(15)	Re(1A)−N(1A)	2.187(12)
Re(1A)−N(3A)	2.161(12)	Re(1A)−N(5A)	2.177(13)
C(1A)−O(1A)	1.187(20)	C(2A)−O(2A)	1.152(25)
C(3A)−O(3A)	1.124(20)	N(5A)−C(4A)	1.126(19)
C(4A)−C(5A)	1.450(20)		
Bond Angles (deg)			
Cation 1			
C(1)−Re(1)−C(2)	87.5(6)	C(1)−Re(1)−C(3)	90.7(7)
C(2)−Re(1)−C(3)	87.0(7)	C(1)−Re(1)−N(1)	171.3(4)
C(2)−Re(1)−N(1)	101.1(5)	C(3)−Re(1)−N(1)	90.8(5)
C(1)−Re(1)−N(3)	97.0(4)	C(2)−Re(1)−N(3)	174.4(6)
C(3)−Re(1)−N(3)	96.2(5)	N(1)−Re(1)−N(3)	74.3(4)
C(1)−Re(1)−N(5)	93.2(6)	C(2)−Re(1)−N(5)	93.0(7)
C(3)−Re(1)−N(5)	176.1(5)	N(1)−Re(1)−N(5)	85.4(5)
N(3)−Re(1)−N(5)	83.6(5)	Re(1)−C(1)−O(1)	173.9(16)
Re(1)−C(2)−O(2)	177.8(19)	Re(1)−C(3)−O(3)	177.0(10)
Re(1)−N(5)−C(4)	176.2(11)	N(5)−C(4)−C(5)	178.7(14)
Cation 2			
C(1A)−Re(1A)−C(2A)	88.5(7)	C(1A)−Re(1A)−C(3A)	87.2(7)
C(2A)−Re(1A)−C(3A)	89.9(7)	C(1A)−Re(1A)−N(1A)	173.2(6)
C(2A)−Re(1A)−N(1A)	98.3(6)	C(3A)−Re(1A)−N(1A)	92.4(6)
C(1A)−Re(1A)−N(3A)	97.9(6)	C(2A)−Re(1A)−N(3A)	172.1(5)
C(3A)−Re(1A)−N(3A)	94.9(6)	N(1A)−Re(1A)−N(3A)	75.4(4)
C(1A)−Re(1A)−N(5A)	95.5(6)	C(2A)−Re(1A)−N(5A)	90.8(6)
C(3A)−Re(1A)−N(5A)	177.2(7)	N(1A)−Re(1A)−N(5A)	84.5(6)
N(3A)−Re(1A)−N(5A)	84.1(4)	Re(1A)−C(1A)−O(1A)	176.2(15)
Re(1A)−C(2A)−O(2A)	178.7(14)	Re(1A)−C(3A)−O(3A)	177.9(14)
Re(1A)−N(5A)−C(4A)	178.1(15)	N(5A)−C(4A)−C(5A)	178.0(21)

Carbonyl Stretching Frequencies. The carbonyl stretching frequencies are listed in Table 4. The tricarbonyl complexes had three infrared-active bands in the 1900−2100 cm^{-1} region which are typical for complexes of this type.[9] The C≡N stretching mode of the acetonitrile adduct is not observed. This absorption normally is located near 2100 cm^{-1}, is very weak,[21] and may be masked by the high-energy CO vibration.

Table 4. CO Vibrational Frequencies for $Re(bpm)(CO)_3L^{n+}$ Complexes[a]

L	ν_{CO} (cm^{-1})[b]		
Cl[c]	2033	1906 (sh)	1899
py	2043 (sh)	2033	1916
CH_3CN	2035	1962 (sh)	1922
MeQ^+	2039	1942 (sh)	1922
py-PTZ	2035	1933	1922

[a] Nujol mulls; 23 ± 2 °C. [b] Errors ±2 cm^{-1}. [c] Reference 9.

Table 5. Ultraviolet–Visible Spectral Data for $Re(bpm)(CO)_3L^{n+}$ Complexes in Acetonitrile[a]

L	$\lambda_{d\pi\rightarrow\pi^*}$, nm ($\epsilon$)[b]		$\lambda_{\pi\rightarrow\pi^*}$, nm ($\epsilon$)[b]	
Cl[c]	364 (2.7)	310 (3.4)	260 (sh)	232 (23)
py		364 (sh)	260 (25)	250 (sh)
CH_{3CN}		357 (sh)		245 (31)
MeQ^+		321 (sh)		249 (32)
py-PTZ		369 (sh)	296 (sh)	255 (48)

[a] $T = 23 \pm 1$ °C. [b] Error in λ ±1.5 nm; molar absorption coefficients $\times 10^{-3}$ M^{-1} cm^{-1}, error ±0.1. [c] Reference 9.

Electronic Absorption Spectra. The results of the UV–visible absorption spectra obtained in acetonitrile are listed in Table 5. The spectra were similar to the one for $Re(bpm)(CO)_3Cl$,[9] and hence, optical transition assignments similar to those already published were made. The most intense bands were located in the 200–300 nm region and assigned as $\pi \rightarrow \pi^*$ transitions centered on the bidentate heterocyclic ligand. The ultraviolet–visible spectrum of $Re(bpm)(CO)_3Cl$ contained two bands in the 300–400 nm region which were assigned as $d\pi \rightarrow \pi^*$ transitions. The bands located in the 300–400 nm region for the tricarbonyl complexes reported here were also assigned as $d\pi \rightarrow \pi^*$ transitions from the metal to the bidentate heterocyclic ligand. There were no assignments made to transitions involving the carbonyl ligands, nor were any transitions to MeQ^+ or py-PTZ distinguishable.

Electrochemistry. Polarographic redox potentials were determined by cyclic voltammetry and are compiled in Table 6. Half-wave potentials ($E_{1/2}$) were deduced by averaging the oxidation and reduction peak potentials for a given redox couple, and reversibility was judged by the difference between them ($E_p = 56$ mV/n, where n is the number of electrons transferred)[22] and the ratio of the oxidation and reduction peak currents, i_{red}/i_{ox} (1 for couples classified as reversible). For the $Re(bpm)(CO)_3L^{n+}$, L = py, CH_3CN, and MeQ^+, there were no observed oxidations out to +2.0 V vs SSCE, indicating that these processes were located outside the potential window of the solvent. However, $Re(bpm)(CO)_3$py-PTZ^+ underwent two oxidations similar to that of the free py-PTZ ligand.[3] For the complex, a reversible, one-electron process was located at 0.82 V and an irreversible process occurred at 1.53 V vs SSCE. The free ligand itself was oxidized reversibly at 0.82 V and irreversibly at 1.57 V vs SSCE. The similarity of the potentials of the complex to those of the free ligand indicates that the oxidations of the complex occur at a remote part of the py-PTZ ligand, which most likely is the phenothiazine moiety,[23,24] as illustrated by eqs 5 and 6.

Reductions of the complexes are less systematic to assign. The first reduction of $Re(bpm)(CO)_3L^{n+}$, L = py, CH_3CN, and py-PTZ, is attributed to reduction of coordinated bpm (eq 7).

$$[Re(bpm)(CO)_3py\text{-}PTZ]^+ - e^- \rightleftharpoons [Re(bpm)(CO)_3py\text{-}PTZ^+]^{2+} \quad (5)$$

$$[Re(bpm)(CO)_3pyPTZ^+]^{2+} - e^- \rightleftharpoons [Re(bpm)(CO)_3py\text{-}PTZ^{2+}]^{3+} \quad (6)$$

$$[Re^I(bpm)(CO)_3CH_3CN]^+ + e^- \rightleftharpoons [Re^I(bpm^-)(CO)_3CH_3CN] \quad (7)$$

The second reduction of $Re(bpm)(CO)_3L^{n+}$, L = CH_3CN and py-PTZ, is irreversible and similar to the electrochemical reductions observed for $Re(bpm)(CO)_3Cl$.[9] For $Re(bpm)(CO)_3Cl$, this reduction was assigned as Re(I) → Re(0) and is thought to be the case here as well (eq 8). However, for $[Re(bpm)(CO)_3py]^+$, rather than an irreversible wave, the second reduction was reversible and assigned as the second reduction of coordinated bpm (eq 9). Coordinated bidentate heterocyclic ligands have been shown to undergo a second one-electron reduction approximately 1 V more negative than the first, which is similar to the result observed here.[25]

$$[Re^I(bpm^-)(CO)_3CH_3CN]^0 + e^- \rightleftharpoons [Re^0(bpm^-)(CO)_3CH_3CN]^- \quad (8)$$

$$[Re(I)(bpm^-)(CO)_3py]^0 + e^- \rightleftharpoons [Re^I(bpm^{2-})(CO)_3py]^- \quad (9)$$

Reduction of $Re^I(bpm)(CO)_3MeQ^{2+}$ can be summarized as follows. The first and third reduction waves (−0.70 and −1.23 V) are attributed to the sequential reduction of the MeQ^+ ligand. These were shifted 30–40 mV in the positive direction compared to that of the free ligand, in accord with the expected positive charge effect upon coordination to Re(I), which lowers the π^* energy levels of coordinated heterocyclic ligands.[26] The second and fourth reduction waves (−0.88 and −1.66 V) are attributed to the sequential reduction of coordinated bipyrimidine. Equations 10–13 illustrate these processes.

$$[Re^I(bpm)(CO)_3MeQ^+]^{2+} + e^- \rightleftharpoons [Re^I(bpm)(CO)_3MeQ^\bullet]^+ \quad (10)$$

$$[Re^I(bpm)(CO)_3MeQ^\bullet]^+ + e^- \rightleftharpoons [Re^I(bpm^-)(CO)_3MeQ^\bullet] \quad (11)$$

$$[Re^I(bpm^-)(CO)_3MeQ^\bullet] + e^- \rightleftharpoons [Re^I(bpm^-)(CO)_3MeQ^{\bullet-}]^- \quad (12)$$

$$[Re^I(bpm^-)(CO)_3MeQ^{\bullet-}]^- + e^- \rightleftharpoons [Re^I(bpm^{2-})(CO)_3MeQ^{\bullet-}]^{2-} \quad (13)$$

Emission Data. Emission data obtained at 77 and 298 K are listed in Table 7. $Re(bpm)(CO)_3L$, L = CH_3CN, py, and MeQ^+, were weak emitters in fluid solution at room temperature. Under similar conditions, no observable emission was found from the complex with L = py-PTZ. The emission spectra were broad, in accord with the ^{3}MLCT assignment of the emission

(21) Sharpe, A. G. *The Chemistry of Cyano Complexes of the Transition Metals*; Academic Press: London, 1976; p 142.
(22) Nicholson, R. S.; Shain, I. *Anal. Chem.* **1964**, *36*, 705.
(23) DeArmond, M. K.; Carlin, C. M. *Coord. Chem. Rev.* **1981**, *36*, 325.
(24) Luong, J. C.; Nadjo, L.; Wrighton, M. S. *J. Am. Chem. Soc.* **1978**, *100*, 5790.
(25) Lindner, E.; Trad, S.; Hoehne, S. *Chem. Ber.* **1980**, *113*, 639.
(26) Callahan, R. W.; Brown, G. M.; Meyer, T. J. *Inorg. Chem.* **1975**, *14*, 1443.

Table 6. Redox Potentials (V) for Re(bpm)(CO)$_3$L^{n+} (L = py, MeQ$^+$, py-PTZ) in Acetonitrile[a]

	oxidation[b]		reduction[b]			
complex	$E_{1/2(2)}$	$E_{1/2(1)}$	$E_{1/2(1')}$	$E_{1/2(2')}$	$E_{1/2(3')}$	$E_{1/2(4')}$
Re(bpm)(CO)$_3$Cl[c]		1.43[d]	−1.03 (70)	−1.65[d]		
Re(bpm)(CO)$_3$py$^+$			−0.84 (65)	−1.82 (70)		
Re(bpm)(CO)$_3$CH$_3$CN$^+$			−0.90 (65)	−1.35[d]		
Re(bpm)(CO)$_3$MeQ^{2+}			−0.70 (65)	−0.86 (65)	−1.29 (65)	−1.66 (90)
Re(bpm)(CO)$_3$py-PTZ$^+$	1.53[d]	0.82(80)	−0.84 (70)	1.41[d]		
bpm[e]			−1.80			
MeQ$^+$			−0.96	−1.66		
py-PTZ	1.57[c]	0.82				

[a] Electrolyte was 0.1 M TBAH; error in potentials was ±0.02 V; T = 23 ± 1 °C; scan rate 200 mV/s; E_p (mV) in parentheses. [b] The numbering sequence is for identification, not assignment of processes. [c] Reference 9. [d] Value is E_p; irreversible. [e] Kawanishi, Y.; Kitimura, E. *Inorg. Chem.* **1989**, *28*, 2968.

Table 7. Emission Data for Re(bpm)(CO)$_3$L^{n+} Complexes in Various Solvents[a]

complex	solvent	$\lambda_{max,77K}$ (nm)	τ_{77K} (ns[b])	$\lambda_{max,298K}$ (nm)	τ_{298K} (ns[b])	Φ_{em} (×1000)[b]
Re(bpm)(CO)$_3$py$^+$	CH$_3$CN			641	2.4	0.58
	CH$_2$Cl$_2$[c]			615	36	2.2
	EtOH/MeOH	556	1019			
Re(bpm)(CO)$_3$CH$_3$CN$^+$	CH$_3$CN			617	4.9	1.9
	CH$_2$Cl$_2$[c]			588	105	5.8
	EtOH/MeOH	578	438			
Re(bpm)(CO)$_3$MeQ^{2+}	CH$_3$CN			625	2.6	0.56
	EtOH/MeOH	556	1010			
Re(bpm)(CO)$_3$py-PTZ$^+$	CH$_3$CN[c,e]			*d*	*d*	*d*
	EtOH/MeOH	558	551			

[a] λ_{ex} = 355 nm, ±1 nm; λ_{max} ± 1 nm; freeze−pump−thaw degassed, unless otherwise noted. [b] Values are ±10%. [c] Under Argon. [d] No emission observed at room temperature. [e] Complex insoluble in CH$_2$Cl$_2$.

for similar rhenium(I) tricarbonyl complexes.[13,27,28] As expected for ^{3}MLCT emitters, the emission maxima were solvent dependent, with λ_{max} in cm^{-1} for a given complex greater in methylene chloride than in acetonitrile. In like manner, emission lifetimes and quantum yields were greater in methylene chloride than in acetonitrile for the same complex.

At 77 K in a 4:1 ethanol/methanol glass, the emission maxima shifted to higher energy and the emission lifetimes increased by 2−3 orders of magnitude. The emission spectra remained broad, and single-exponential decays were observed.

A comparison of the emission properties in Table 7 of Re(bpm)(CO)$_3$MeQ^{2+} to those of Re(bpm)(CO)$_3$py$^+$ reveals very similar photophysical characteristics. However, emission from Re(bpm)(CO)$_3$py-PTZ$^+$ is quenched, except at low temperature in an ethanol/methanol glass. A comparison of the emission properties of Re(bpm)(CO)$_3$(CH$_3$CN)$^+$ to Re(bpm)(CO)$_3$py$^+$ reveals that the acetonitrile adduct has 2−3 times larger emission lifetime and quantum yield than those of the pyridine adduct.

Transient Absorption Spectra. Transient absorption spectra and lifetimes were examined by both picosecond and nanosecond laser flash photolysis due to the fact that most of the observed transients had kinetic and spectral features that fell between these time regimes. Consequently, collection of data was challenging and transient spectra and lifetimes were necessarily constructed from both of these sources.

Irradiation of Re(bpm)(CO)$_3$py$^+$, the control, at 355 nm in CH$_3$CN resulted in the spectral profile shown in Figure 3 consisting of a sharp, intense peak centered at 350 nm and a broad peak of approximately half the intensity centered at 425 nm. Both spectral features were present immediately after the nanosecond laser pulse and followed the same decay kinetics

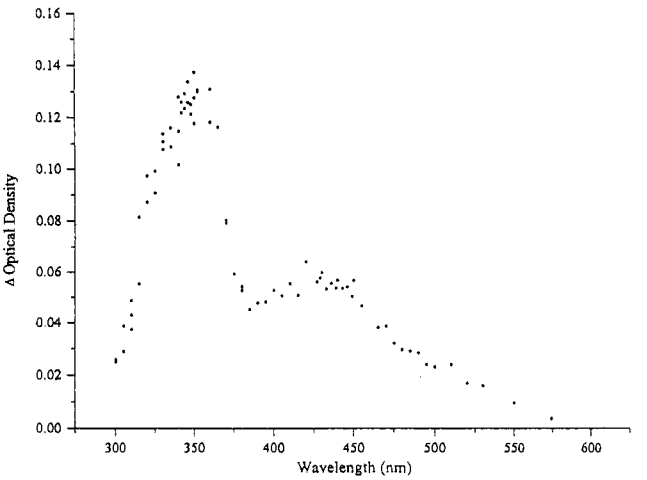

Figure 3. Transient absorption spectrum of Re(bpm)(CO)$_3$py$^+$ 1.56 ns after the 355 nm flash. The solvent was acetonitrile, and the temperature was ambient.

within the resolution of the nanosecond spectrophotometer. This method put an upper limit of $\tau \leq 20$ ns on these transients.

When the pyridine ligand was replaced with the electron acceptor MeQ$^+$, the transient absorption spectrum shown in Figure 4 contained the features found for the pyridine analog at 350 and 450 nm along with a broad absorbance centered at 640 nm. As in the previous case, the transients were present immediately after the laser pulse and the temporal profiles of all three features were the same within the time resolution of the nanosecond spectrometer. Picosecond flash measurements, on the other hand, showed that these two features at 450 and 650 nm relaxed with τ = 18 ns.

When the pyridine ligand was replaced by the electron-donating py-PTZ ligand, short-lived transients shown in Figure 5 were observed. As in the previous cases, a sharp, intense UV absorption was found, but shifted to higher energy, λ_{max} = 335 nm. Unlike the case of previous molecules, the 450 nm

(27) (a) Tapolsky, G.; Duesing, R.; Meyer, T. J. *J. Phys. Chem.* **1989**, *93*, 2885. (b) Tapolsky, G.; Duesing, R.; Meyer, T. J. *Inorg. Chem.* **1990**, *29*, 2285.

(28) (a) Hino, J. K.; Della Ciana, L.; Dressick, W. J.; Sullivan, B. P. *Inorg. Chem.* **1992**, *31*, 1072. (b) Della Ciana, L.; Dressick, W. J.; Sandrini, D.; Maestri, M.; Ciano, M. *Inorg. Chem.* **1990**, *29*, 2792.

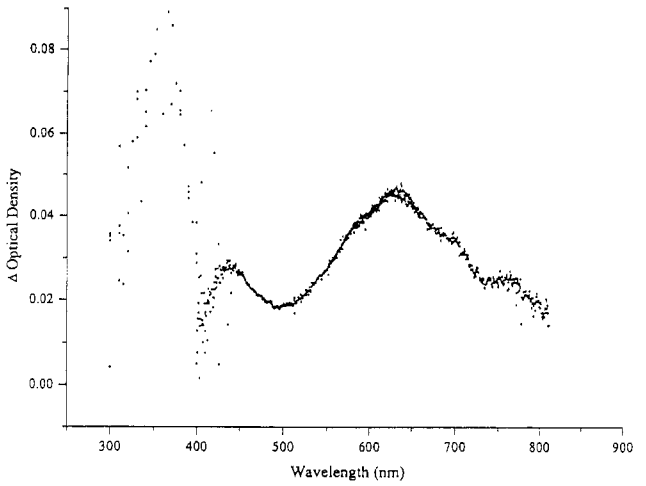

Figure 4. Transient absorption spectrum of $Re(bpm)(CO)_3MeQ^{2+}$ 1.56 ns after the 355 nm flash. The solvent was acetonitrile, and the temperature was ambient. The spectrum is a superposition of the nanosecond and picosecond results, where the picosecond results are represented by the solid line and the nanosecond results by the unlined dots.

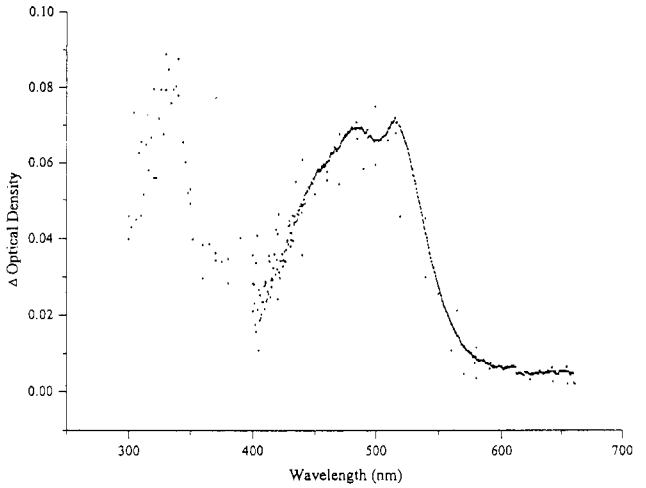

Figure 5. Transient absorption spectrum of $Re(bpm)(CO)_3py\text{-}PTZ^+$ 1.56 ns after the 355 nm flash. The solvent was acetonitrile, and the temperature was ambient. The spectrum is a superposition of the nanosecond and picosecond results, where the picosecond results are represented by the solid line and the nanosecond results by the unlined dots.

absorbance, if present, was obscured by the presence of the absorbance of the py-PTZ radical which had maxima at 475 and 516 nm. The time dependence of the UV and visible absorbances followed the nanosecond laser pulse. On the picosecond time scale, however, this latter absorbance was observed to have a rise time of ~900 ps and decayed with τ = 6 ns. We were unable to ensure that the UV absorbance followed the same kinetic behavior since the picosecond spectrometer was blind below 400 nm. However, these results are similar to those reported for $Re(bpy)(CO)_3py\text{-}PTZ$.[3]

Discussion

Preparation of Compounds. Previous synthetic schemes for preparing rhenium(I) tricarbonyl heterocyclic ligand complexes involved either reacting $Re(CO)_5Cl$ directly with L-L, where L-L is a bidentate heterocyclic ligand, to yield $Re(L\text{-}L)(CO)_3Cl$[9-13,29-32] or reacting $Re(CO)_5L$, where L is an anionic ligand such as $CF_3SO_3^+$, with L-L to yield $Re(L\text{-}L)(CO)_3L^+$. The approach taken here was to prepare $Re(CO)_3(CH_3OH)_3^+$ by refluxing $Re(CO)_5Cl$ in methanol and following this by reaction with 2,2′-bipyridmidine (bpm) to produce $Re(bpm)(CO)_3(CH_3OH)^+$. This was isolated as the PF_6^- salt, redissolved in methylene chloride containing MeQ^+ or py-PTZ. The methanol was displaced by MeQ^+ or py-PTZ, resulting in formation of $Re(bpm)(CO)_3MeQ^{2+}$ or $Re(bpm)(CO)_3(py\text{-}PTZ)^+$, respectively.

Structures. The X-ray stuctures of three $Re^I(bpm)(CO)_3L^{n+}$ complexes, where L = CO,[33] CH_3CN,[34] and MeQ^+,[34] can be compared and related to their photophysical properties. The Re−N(bpm) bond distances for the three complexes ranged from 2.15 to 2.19 Å. The Re−C(CO) bond distances were similar (~1.94 Å), except for $Re(bpm)(CO)_4^+$, where the bond distances to the CO ligands *trans* to one another were 2.09 Å. The major difference within the coordination sphere of the three complexes were the Re to L bond distances which had values of 2.03 Å (Re−CO), 2.14 Å (Re−CH_3CN), and 2.21 Å (Re−MeQ^+). The bond distances correlate with the emission energy maxima in acetonitrile at room temperature, which fell in the respective order 543 nm (Re−CO), 617 nm (Re−CH_3CN), and 625 nm (Re−MeQ^+). One structural feature exhibited by the L = MeQ^+ complex was different from the others due to the molecular structure of the ligand itself. The conjugation about the py−$pyCH_3^+$ bond of the MeQ^+ ligand was broken by a 38° rotation.[34] This break in conjugation affects intramolcular electron transfer as noted below.

Emission. The emission spectra of $Re(bpm)(CO)_3L$, where L is CH_3CN, py, and MeQ^+, were broad and unstructured at both room temperature and 77 K. The spectra were similar to those of other rhenium(I) tricarbonyl complexes classified as ^{3}MLCT emitters.[13,27,28] The emission maxima at room temperature in acetonitrile fell in the order 641 nm for $[Re(bpm)(CO)_3py]^+$, 625 nm for $[Re(bpm)(CO)_3MeQ]^{2+}$, and 617 nm for $[Re(bpm)(CO)_3(CH_3CN)]^+$, putting the ^{3}MLCT state ~2.0 ± 0.2 eV above the ground state. At 77 K, all four complexes emit, including the py-PTZ derivative. Their emission maxima were shifted to higher energies compared to the results at room temperature and fell in the order 578 nm ($[Re(bpm)(CO)_3(CH_3CN)]$) > 558 nm ($[Re(bpm)(CO)_3py\text{-}PTZ]^+$) ~ 556 nm ($[Re(bpm)(CO)_3MeQ]^{2+}$) ~ 556 nm ($[Re(bpm)(CO)_3py]^+$). A temperature-dependent blue shift is commonly observed for ^{3}MLCT emitters which results from nonequilibration of the emitting state with respect to the solvent environment and geometry of the complex.[12] The presence of the py-PTZ group leaves the photophysical characteristics of the emitting state unaffected at 77 K but quenches the emission in fluid solution.

Quenching of emission in $Re(bpm)(CO)_3MeQ^{2+}$ and $Re(bpm)(CO)_3py\text{-}PTZ^+$ was anticipated due to the presence of intervening ligand states between the ground and excited states. For the MeQ^+ and py-PTZ derivatives, the electrochemical results

(29) (a) Lin, R.; Guarr, T. F. *Inorg. Chim. Acta* **1990**, *167*, 149. (b) Lin, R.; Guarr, T. F.; Duesing, R. *Inorg. Chem.* **1990**, *29*, 4169.

(30) (a) Caspar, J. V.; Sullivan, B. P.; Meyer, T. J. *Inorg. Chem.* **1984**, *23*, 2098. (b) Kober, E. M.; Marshall, J. L.; Dressick, W. J.; Sullivan, B. P.; Meyer, T. J. *Inorg. Chem.* **1985**, *24*, 2755. (c) Kober, E. M.; Sullivan, B. P.; Dressick, W. J.; Caspar, J. V.; Meyer, T. J. *J. Am. Chem. Soc.* **1980**, *102*, 1383.

(31) (a) Wrighton, M. S.; Morse, D. L. *J. Am. Chem. Soc.* **1974**, *96*, 998. (b) Giordano, P. J.; Fredericks, S. M.; Wrighton, M. S.; Morse, D. L. *J. Am. Chem. Soc.* **1978**, *100*, 2257. (c) Giordano, P. J.; Wrighton, M. S. *J. Am. Chem. Soc.* **1979**, *101*, 2888. (d) Fredericks, S. M.; Luong, J. C.; Wrighton, M. S. *J. Am.Chem. Soc.* **1979**, *101*, 7415. (e) Smothers, W. K.; Wrighton, M. S. *J. Am. Chem. Soc.* **1983**, *105*, 1067.

(32) Vogler, A.; Kisslinger, J. *Inorg. Chim. Acta* **1986**, *115*, 193.

(33) Shaver, R. J.; Rillema, D. P.; Woods, C. *J. Chem. Soc., Chem. Commun.* **1990**, 179.

(34) Winslow, L. N.; Rillema, D. P.; Welch, J. H.; Singh, P. *Inorg. Chem.* **1989**, *28*, 1596.

Scheme 2. Arrangement of the Empty MeQ$^+$ Orbital and the Filled py-PTZ Orbital Relative to the Emission Energy

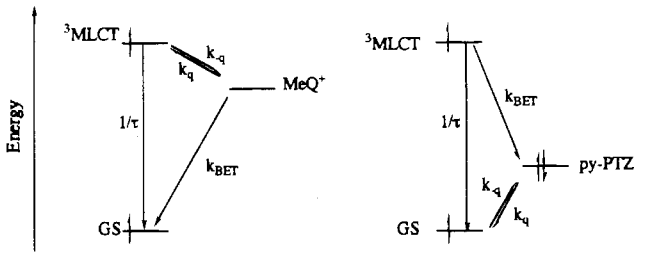

allow one to estimate the placement of the unoccupied state of MeQ$^+$ to be approximately 0.15V below the emitting ^{3}MLCT state and the filled py-PTZ state to be approimately 0.70 V above the ground state. This is illustrated in Scheme 2. While emission quenching at room temperature was observed for Re(bpm)(CO)$_3$py-PTZ$^+$, Re(bpm)(CO)$_3$MeQ^{2+} behaved like the control, Re(bpm)(CO)$_3$py$^+$. Thus, $k_q \gg 1/\tau$ for Re(bpm)(CO)$_3$-py-PTZ$^+$, whereas the opposite is true for Re(bpm)(CO)$_3$MeQ^{2+}, $1/\tau \gg k_q$.

Charge Separation. The transient species form and decay rapidly, making it difficult to obtain accurate rate constants in most cases. Nevertheless, the results obtained are meaningful with respect to the behavior of excited states in bpm complexes. Each case is different and will be considered separately:

Re(bpm)(CO)$_3$py$^+$ The transient absorption characteristics illustrated in Figure 3 can be interpreted to arise from the product presented in eq 14. The absorbance at 350 nm is attributed to

$$Re^I(bpm)(CO)_3py^+ \underset{\tau^{-1}}{\overset{h\nu}{\rightleftharpoons}} Re^{II}(bpm^-)(CO)_3py^{+*} \quad (14)$$

the bpm$^-$ radical and the one at 425 nm is tentatively assigned to the presence of Re(II). The assignment of the higher energy transition to the bpm$^-$ radical, is consistent with the 370 nm assignment reported[3] for bpy$^-$ in Re^{II}(bpy$^-$)(CO)$_3$(Etpy)$^+$, where Etpy is 4-ethylpyridine. The broad absorbance at 425 nm is also observed in Re^{II}(bpy$^-$)(CO)$_3$Etpy^{+*} and appears characteristic of Re(II) in charge-separated species. The irreversibility of the oxidation to form "Re^{II}(L-L)" species, where L-L is a bidentate ligand, precludes electrochemical oxidation as a means for obtaining additional proof with respect to this hypothesis.

The formation of Re^{II}(bpm$^-$)(CO)$_3$py^{+*} and its decay occur within the laser pulse. We estimate its formation to occur in $>10^{-12}$ s on the basis of the rise time of the laser pulse. Its lifetime can be estimated from luminescence measurements. A value of $\tau \sim 2.4 \times 10^{-9}$ s was obtained by single-photon-counting luminescence measurements.

The short-lived transient is consistent with the energy gap[35,36] law. Electrochemically the reduction of bpm indicates that the energy gap is decreased by approximately 0.5V compared to the analogous bpy complex and thereby increases k_{nr}. Thus, a decrease in the lifetime of the Re^{II}bpm$^-$ transient compared to the Re^{II}bpy transient is expected.

Re(bpm)(CO)$_3$py-PTZ$^+$. When L is replaced by the electron donor py-PTZ, a behavior different from the one above where L = py is observed. The first *thexi* state in this molecule is attributed to Re(I) → bpm charge transfer (Scheme 3). But, unlike the case where L = py, other processes are energetically accessible. A process involving electron transfer from a filled

Scheme 3. Reactivity Sequences of Photoexcited Re^I(bpm)(CO)$_3$(py-PTZ)$^+$

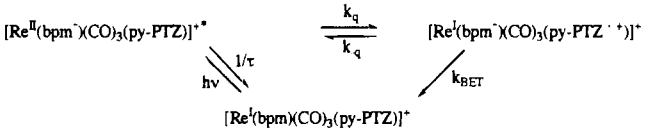

Scheme 4. Reactivity Sequences of Photoexcited Re^I(bpm)(CO)$_3$MeQ^{2+}

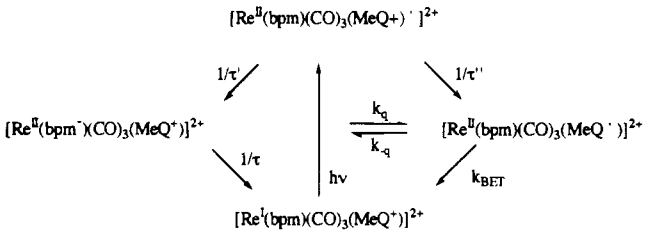

orbital on the py-PTZ ligand to the hole in the d orbital on Re vacated by optical absorption should have a driving force of ≥0.8 V on the basis of electrochemical measurements of the oxidation of free py-PTZ. Consistent with this, we see transients at 475 and 516 nm that appear within 900 ps after the flash ($k_q \gg 1/\tau$). The peak associated with bpm$^-$ has blue-shifted by 25 nm, in accord with the $\pi-\pi^*$ character of bpm$^-$ attached to Re(I) rather than Re(II). Both spectral features are consistent with the formation of Re^I(bpm$^-$)(CO)$_3$(py-PTZ$^+$)$^+$. This charge-separated species then underwent intraligand electron transfer (ILCT) at a rate of $k_{BET} = 1.6 \times 10^8$ s^{-1}. The value of k_{BET} is consistent with work of Wasielewski.[37]

Re(bpm)(CO)$_3$MeQ^{2+}. Scheme 4 can be used to account for the photophysical properties and the transient absorptions of Re(bpm)(CO)$_3$MeQ^{2+} found in Figure 6. As for Re(bpm)-(CO)$_3$py$^+$, transient absorptions appeared within the laser pulse. The one at 350 nm is derived from bpm$^-$ attached to Re(II), the one at 450 nm is tentatively assigned to Re(II), and the one at 625 nm is related to absorption by MeQ$^{\cdot}$.[38] The presence of this radical stands in marked contrast to the emission results, where no quenching by MeQ$^+$ in Re(bpm)(CO)$_3$MeQ$^+$ was observed. Therefore, to account for the overall photophysical observations, it is necessary to invoke population of an excited state which can partition its energy between two lower energy excited states, one related to [Re^{II}(bpm$^-$)(CO)$_3$(MeQ$^+$)]$^{2+}$ and the other assigned to [Re^{II}(bpm)(CO)$_3$(MeQ$^{\cdot}$)]$^{2+}$. This certainly is plausible, given the fact that initial excitation occurs to the ^{1}MLCT state, the fact that there is a high density of excited states, and the fact that the energy of separation between Re^I(bpm$^-$) and Re^I(MeQ$^{\cdot}$) is small, which likely carries over to the excited state species. Thus, the initial *thexi* state for this molecule may not be well defined or may involve an equilibrium between the two closely spaced Re^{II}(bpm$^-$) and Re^{II}(MeQ$^{\cdot}$) singlet states. Once both species are formed, the dominant mode of decay is to fill the hole on Re(II) by electron transfer from the attached radical due to the large driving force of ~2 V. Intramolecular ligand charge transfer represented by k_q and k_{-q} does not seem to occur. Thus, [Re^{II}(bpm$^-$)(CO)$_3$(MeQ$^+$)]$^{2+*}$ decays by emission ($\tau = 2.6$ ns) at approximately the same rate as [Re^{II}(bpm$^-$)(CO)$_3$py]$^{+*}$ ($\tau = 2.4$ ns). [Re^{II}(bpm)(CO)$_3$-

(35) Allen, G.; Rillema, D. P.; Meyer, T. J.; White, R. P. *J. Am. Chem. Soc.* **1984**, *106*, 2613.
(36) (a) Caspar, J. V.; Meyer, T. J. *J. Phys. Chem.* **1983**, *87*, 952. (b) Caspar, J. V.; Meyer, T. J. *Inorg. Chem.* **1983**, *22*, 2444. (c) Caspar, J. V.; Kober, E. M.; Sullivan, B. P.; Meyer, T. J. *J. Am. Chem. Soc.* **1982**, *104*, 630.
(37) (a) Wasielewski, M. R.; Niemczyk, M. P.; Svec, W. A.; Pewitt, E. B. *J. Am. Chem. Soc.* **1985**, *107*, 1080. (b) Wasielewski, M. R.; Johnson, D. G.; Svec, W. A. Photoinduced Electron Transfer in Fixed Distance Chlorophyll-quinone Donor-Acceptor Molecules. In *Supra Molecular Photochemistry*; Balzani, V., Ed.; Kluwer: Dordrecht, 1987.
(38) Sullivan, B. P.; Abruna, H. D.; Finklea, H. O.; Salmon, D. J.; Nagle, J. K.; Meyer, T. J.; Sprintschnik, H. *Chem. Phys. Lett.* **1978**, *58*, 389.

$(MeQ^{\bullet})]^{2+}$ decays a little less rapidly by back electron transfer, $k_{BET} = 5.5 \times 10^7\ s^{-1}$. This inhibition may be the result of a structural problem. Crystal structure studies have shown the *N*-methylpyridine unit in MeQ^+ to be noncoplaner with the pyridine functionality.[34] This structural feature may decrease overlap of the appropriate orbitals used in the electron transfer process and thereby decrease the rate of the electron transfer reaction.

Conclusion. A clearer understanding of the photophysical features leading to charge separation in rhenium(I) polypyridyl systems emerges. First, emission occurs from a low-lying excited state with properties resembling those of the ^{3}MLCT state. Emission from this state is broad and structureless. The rise time in the flash photolysis results for $[Re^{I}(bpm)(CO)_3py\text{-}PTZ]^+$, conversion of $[Re^{II}(bpm^-)(CO)_3py\text{-}PTZ]^+$ to $[Re^{I}(bpm^-)(CO)_3(py\text{-}PTZ^+)]^+$, is associated with emission quenching from this state. Lying above this state is another state, postulated to be a ^{1}MLCT state, which is a necessary upper excited state to invoke in order to account for the photophysics of $[Re(bpm)(CO)_3(MeQ^+)]^{+,2+*}$. Second, intraligand charge transfer in $[Re^{II}(bpm^-)(CO)_3\ (MeQ^+)]^{2+*}$ to form $[Re^{II}(bpm)(CO)_3(MeQ)^{\bullet}]^{2+*}$ does not seem to occur due to quenching by a more energetic pathway, reduction of Re(II) to Re(I). Emission quenching by MeQ^+ was not observed for this complex.

Acknowledgment. We thank the Office of Basic Energy Sciences of the U.S. Department of Energy for support. D.P.R. and M.W.P. acknowledge a Dreyfus Scholar/Fellow Award. We thank Dr. Larry Patterson at the Notre Dame Radiation Laboratory for the use of his single-photon-counting equipment and the Notre Dame Radiation Laboratory for use of their picosecond and nanosecond laser flash photolysis systems. We also thank Dr. Guillermo Ferraudi for his assistance and hosting our visits to NDRL.

Supporting Information Available: Tables listing crystal data and data collection, solution, and refinement parameters, bond lengths, bond angles, anisotropic displacement coefficients, and H atom coordinates and isotropic displacement coefficients (8 pages). Ordering information is given on any current masthead page.

IC950323+